Inorg. Chem. **2008**, *47*, 1007–1019

Salts of Methylated 5-Aminotetrazoles with Energetic Anions

Konstantin Karaghiosoff, Thomas M. Klapötke,* Peter Mayer, Carles Miró Sabaté, Alexander Penger, and Jan M. Welch

Department of Chemistry and Biochemistry, Ludwig-Maximilians-Universität München, Butenandtstrasse 5-13, D-81377 München, Germany

Received September 17, 2007

1-Methyl-5-aminotetrazole (**4**, MAT) can easily be protonated by strong acids, yielding known but largely uninvestigated 1-methyl-5-aminotetrazolium nitrate (**4a**) and perchlorate (**4b**). Methylation, rather than protonation, of **4** with iodomethane followed by the exchange of the iodide (**5a**) for nitrate (**5b**), perchlorate (**5c**), azide (**5d**), and dinitramide (**5e**) yields a new family of energetic methylated aminotetrazole salts. In all cases, stable salts were obtained and fully characterized by vibrational (IR, Raman) spectroscopy, multinuclear NMR spectroscopy, mass spectrometry, elemental analysis, and X-ray structure determination. Compounds **4a**, **4b**, and **5c** crystallize in the monoclinic space group $P2_1/n$, whereas compounds **5b** and **5e** crystallize in the orthorhombic space group $P2_12_12_1$ and **5d** in the orthorhombic *Fddd*. Initial safety testing (impact, friction, and electrostatic sensitivity) and thermal stability measurements (DSC) were also carried out. The MAT salts all exhibit good thermal stabilities (decomposition above 150 °C). The constant volume energies of combustion ($\Delta_c U$) of **4a**, **5b**, **5d**, and **5e** were determined to be –2510(10) cal/g, –3190(30) cal/g, –4500(100) cal/g, and –2570(70) cal/g, respectively, experimentally using oxygen bomb calorimetry. From the experimentally determined density, chemical composition and energies of formation (back calculated from the heats of combustion), the detonation pressures and velocities of **4a** (8100 m/s, 25.6 GPa), **5b** (7500 m/s, 20.2 GPa), **5d** (8200 m/s, 21.7 GPa), and **5e** (7500 m/s, 21.2 GPa) were predicted using the EXPLO5 code.

Introduction

In the development of energetic materials, increased performance with decreased sensitivity to physical stimuli is sought. Unfortunately, performance and sensitivity are linked both to each other and to general physical and chemical properties, most significantly enthalpy of formation (ΔH_f), density (ρ), and oxygen balance (Ω). One way of counteracting the correlation of high performance (detonation pressure and detonation velocity) with high sensitivity to impact, friction, and shock is the use of systems such as 1,1-diamino-2,2-dinitroethene (FOX-7)[1] or 1,3,5-triamino-2,4,6-trinitrobenzene,[2] which form extensive hydrogen-bonding networks in the solid state. Such hydrogen-bonded networks (especially between amino and nitro groups) help to stabilize the material substantially. In addition to lower sensitivities, the performance of such materials is generally adequate since chemical composition (FOX-7, for example, shares a common empirical formula, $CH_2N_2O_2$, with HMX and RDX) is unaffected by strong hydrogen bonding, density is generally increased and heat of formation slightly decreased (less positive). Since the performance of an energetic material is most heavily dependent on density, increases in density tend to outweigh the adverse affect on heat of formation caused by strong hydrogen bonding.[3] The density of such materials often benefits from the higher packing efficiency achieved through stronger intermolecular interactions.

Ionic energetic materials based on aminotetrazoles are also known to form strong hydrogen-bonding networks and thus show remarkable stability and considerable insensitivity to physical stimuli as well as good performance. In addition, known aminotetrazole salts are composed mainly of nitrogen and thus have large positive enthalpies of formation as well as densities comparable to or greater than those of widely used neutral, covalent, organic explosives. The oxygen balances of such salts are only slightly negative when an oxygen-rich counteranion (perchlorate, nitrate, and dinitra-

* Author to whom correspondence should be addressed. E-mail: tmk@cup.uni-muenchen.de. Fax: +49 89 2180 77492.

(1) Bemm, U.; Östmark, H. *Acta Crystallogr.* **1998**, *C54*, 1997−1999.
(2) Cady, H. H.; Larson, A. C. *Acta Crystallogr.* **1965**, *18*, 485−496.
(3) Koehler, J.; Meyer, R. *Explosivstoffe*, 9th ed.; Wiley-VCH: Weinheim, Germany, 1998.

10.1021/ic701832z CCC: $40.75
Published on Web 12/29/2007

mide) is used. Furthermore, ionic energetic materials tend to exhibit lower vapor pressure (essentially eliminating the risk of exposure through inhalation) than similar neutral nonionic analogues.[4] With these properties in mind, aminotetrazole-based compounds have long been of interest as potential energetic materials.[5] Recently, the synthesis and properties of several new classes of heterocycle-based (tetrazole and triazole) energetic salts have been reported.[6] In addition to recent interest, many common (and classic) propellant and explosive compositions are based on oxygen-rich ionic materials including ammonium and potassium perchlorate and nitrate and ammonium dinitramide.

Salts of 5-amino-1*H*-tetrazole **1** (5-AT) and 1,5-diamino-1*H*-tetrazole **2** (DAT) have been investigated in our research group but suffer several shortcomings. First, in the case of DAT salts, synthesis of the parent compound is difficult and hazardous.[7] Second, in spite of their large number of electron pairs, **1** and **2** are both only weakly basic and therefore are only protonated by strong acids, thus precluding their direct combination with several slightly basic nitrogen and oxygen rich anions (e.g., dinitramide and azide). Therefore, in the case of **2**, the tetrazole ring was selectively methylated at the N4 position, generating the protonated form of **3** with no strongly acidic protons and allowing for combination with a far greater variety of anions. Therefore, we chose to investigate combinations of methylated salts of **1** with classic energetic and oxidizing anions (ClO_4^-, NO_3^-, N_3^-, $(NO_2)_2N^-$).

Monomethylation of **1** (or an alkali metal salt of **1**) is known to yield a mixture of **4** and 2-methyl-5-aminotetrazole with **4** as the favored isomer.[8] Both of these isomers may be protonated by strong mineral acids or methylated further. Though a small number of salts (namely hydrohalides) of monomethylated and polymethylated 5-aminotetrazoles are known,[9] the only potentially energetic salts found in the literature are the nitrate[10] and picrate[11] of **4** and the picrate[9b] and nitrate[6b] of 1,4-dimethyl-5-iminotetrazole (**5**). However, the physical and energetic properties of the known nitrates remain largely unknown, and the potential of polymethylated tetrazolium cations remains unclear. Here we present the syntheses, characterization, and initial investigations into thermal and energetic properties of a series of salts based on **4** and **5**.

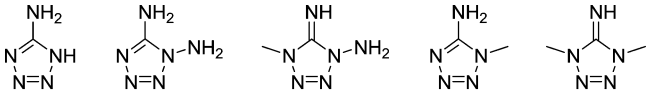

Experimental Section

Caution! Although we experienced no difficulties with the compounds described here, silver azide, dinitramides, aminotetrazoles, and their derivatives are energetic materials and tend to explode under certain conditions. Appropriate safety precautions should be taken, especially when these compounds are prepared on a larger scale. Laboratories and personnel should be properly grounded, and safety equipment such as Kevlar gloves, leather coats, face shields, and ear plugs are highly recommended.

General. All chemical reagents and solvents were obtained from Sigma-Aldrich Inc. or Acros Organics (analytical grade) and were used as supplied. Silver azide and silver bis-pyridine dinitramide[12] were prepared according to known procedures. ^1H, ^{13}C, and ^{15}N NMR spectra were recorded on a JEOL Eclipse 400 instrument in DMSO-d_6 at or near 25 °C. The chemical shifts are given relative to tetramethylsilane (^1H, ^{13}C) or nitromethane (^{15}N) as external standards, and coupling constants are given in hertz (Hz). Infrared (IR) spectra were recorded on a Perkin-Elmer Spectrum One FT-IR instrument as KBr pellets at 20 °C. Transmittance values are qualitatively described as "very strong" (vs), "strong" (s), "medium" (m), and "weak" (w). Raman spectra were recorded on a Perkin-Elmer Spectrum 2000R NIR FT-Raman instrument equipped with a Nd:YAG laser (1064 nm). The intensities are reported as percentages of the most intense peak and are given in parentheses. Elemental analyses were performed with a Netsch Simultaneous Thermal Analyzer STA 429. Melting points were determined by differential scanning calorimetry (Perkin-Elmer Pyris 6 DSC instrument, calibrated with standard pure indium and zinc). Measurements were performed at a heating rate of 10 °C/min in closed aluminum sample pans with a 1 μm hole in the top for gas release under a nitrogen flow of 20 mL/min with an empty identical aluminum sample pan as a reference.

Bomb Calorimetry. For all calorimetric measurements, a Parr 1356 bomb calorimeter (static jacket) equipped with a Parr 207A oxygen bomb for the combustion of highly energetic materials was used.[13] A Parr 1755 printer, furnished with the Parr 1356 calorimeter, was used to produce a permanent record of all activities within the calorimeter. The samples (~200 mg each) were carefully mixed with ~800 mg analytical grade benzoic acid and pressed into pellets, which were subsequently burned in a 3.05 MPa atmosphere of pure oxygen. The experimentally determined heats of combustion were obtained as the averages of five single measurements with standard deviations calculated as a measure of experimental uncertainty. The calorimeter was calibrated by the combustion of certified benzoic acid in an oxygen atmosphere at a pressure of 3.05 MPa.

Synthesis of 1-Methyl-5-aminotetrazole (4). Compound **4** prepared according to literature:[14] mp 226−229 °C; IR (KBr, cm^{-1}) ν 3328(s), 3151(s), 2950(w), 2805(w), 2741(w), 2454(w), 2380-(w), 2262(w), 2203(w), 2157(w), 1679(s), 1666(s), 1595(s), 1483-

(4) (a) Xue, H.; Shreeve, J. M. *Adv. Mater.* **2005**, *17*, 2142−2146. (b) Xue, H.; Twamley, B.; Shreeve, J. M. *Inorg. Chem.* **2005**, *44*, 7009−7013. (c) Sikder, A. K.; Sikder, N. *J. Haz. Mater.* **2004**, *A112*, 1−15.
(5) (a) Gálvez-Ruiz, J. C.; Holl, G.; Karaghiosoff, K.; Klapötke, T. M.; Löhnwitz, K.; Mayer, P.; Nöth, H.; Polborn, K.; Rohbogner, C. J.; Suter, M.; Weigand, J. J. *Inorg. Chem.* **2005**, *44*, 4237−4253. (b) v. Denffer, M.; Klapötke, T. M.; Kramer, G.; Spiess, G.; Welch, J. M.; Heeb, G. *Propellants, Explos., Pyrotech.* **2005**, *30*, 191−195. (c) Klapötke, T. M.; Karaghiosoff, K.; Mayer, P.; Penger, A.; Welch, J. M. *Propellants, Explos., Pyrotech.* **2006**, *31*, 188−195.
(6) (a) Singh, R. P.; Verma, R. D.; Meshri, D. T.; Shreeve, J. M. *Angew. Chem., Int. Ed.* **2006**, *45*, 3584−3601. (b) Wang, R.; Gao, H.; Ye, C.; Twamley, B.; Shreeve, J. M. *Inorg. Chem.*, **2007**, *46*, 932−938.
(7) Gálvez-Ruiz, J. C.; Holl, G.; Karaghiosoff, K.; Klapötke, T. M.; Löhnwitz, K.; Mayer, P.; Nöth, H.; Polborn, K.; Rohbogner, C. J.; Suter, M.; Weigand, J. J. *Inorg. Chem.* (Addition/Correction) **2005**, *44*, 5192.
(8) Spear, R. J. *Aust. J. Chem.*, **1984**, *37*, 2453−2468.
(9) (a) Percival, D. F.; Herbst, R. M. *J. Org. Chem.* **1957**, *22*, 925−933. (b) Henry, R. A.; Finnegan, W. G.; Lieber, E. *J. Am. Chem. Soc.* **1954**, *76*, 2894−2898. (c) Bryden, J. H. *Acta. Crystallogr.* **1957**, *10*, 148.
(10) Garrison, J. A.; Herbst, R. M. *J. Org. Chem.* **1957**, *22*, 278−283.
(11) Lyakhov, A. S.; Voitekhovich, S. V.; Ivashkevich, L. S.; Gaponik, P. N. *Acta Crystallogr.* **2005**, *E61*, o3645−o3647.
(12) Ang, H.-G.; Fraenk, W.; Karaghiosoff, K.; Klapötke, T. M.; Mayer, P.; Nöth, H.; Sprott, J.; Warchhold, M. *Z. Anorg. Allg. Chem.* **2002**, *628*, 2894−2900.
(13) http://www.parrinst.com.

(m), 1321(m), 1279(w), 1236(w), 1121(w), 1090(m), 1043(w), 970(w), 789(m), 742(w), 688(w), 679(m), 538(w); Raman (200 mW, 25 °C, cm^{-1}) ν 3150(13), 3042(5), 2951(32), 2888(4), 2809-(4), 1661(13), 1594(20), 1484(10), 1411(13), 1319(28), 1278(22), 1119(17), 1093(10), 1043(8), 973(7), 789(100), 680(19), 478(10), 313(23), 218(16); ^{1}H NMR (DMSO-d_6, 25 °C) δ 6.65 (s, NH_2), 3.70 (s, CH_3); ^{13}C NMR (DMSO-d_6, 25 °C) δ 156.4 (C_{arom}), 32.0 (CH_3); ^{15}N NMR (DMSO-d_6, 25 °C) δ 2 (N2, q, ^3J = 1.5 Hz), −23 (N3), −93 (N4, t, ^2J = 1.5 Hz), −185 (N1, q, ^2J = 1.7 Hz), −339 (N5, t, ^1J = 87.0 Hz); MS (EI+, 70 eV, >5%) m/z (%) 100(10) [M+], 99(100) [M+], 57(29), 43(90), 42(77), 28(60), 27-(14), 15(34); $C_2H_5N_5$ (99.01) calcd: C 24.2, H 5.1, N 70.7%; found: C 24.2, H 5.0, N 70.5%.

Synthesis of 1-Methyl-5-aminotetrazolium Nitrate (4a).[10] To 2 mL of concentrated nitric acid was added 1.620 g (10.0 mmol) of solid crystalline **4**. The clear, colorless reaction mixture was stirred until all **4** had dissolved. The solution was then cooled to 4 °C overnight, resulting in the formation of clear colorless crystals suitable for X-ray analysis, which were filtered off cold and washed until dry and acid free with diethyl ether. No further purification was necessary (1.206 g, 7.4 mmol, 74%): mp 162−164 °C; IR (KBr, cm^{-1}) ν 3357(s), 3306(s), 3236(s), 3159(s), 2873(w), 2623-(b), 2358(b), 1760(w), 1687(s), 1487(w), 1363(s), 1312(s), 1256-(s), 1231(s), 1088(w), 1032(m), 965(m), 901(w), 775(w), 716(m); Raman (200 mW, 25 °C, cm^{-1}) ν 2961(22), 1685(11), 1597(8), 1515(10), 1426(21), 1273(17), 1049(100), 778(89), 717(16), 665-(18), 461(14), 302(22), 230(18), 136(25); ^{1}H NMR (DMSO-d_6, 25 °C) δ 9.1 (s, N-H, NH_2), 3.9 (s, CH_3); ^{13}C NMR (DMSO-d_6, 25 °C) δ 153.6 (C_{arom}), 32.9 (CH_3); ^{15}N NMR (DMSO-d_6, 25 °C) δ −11.5 (N6), −13.5 (N3), −24.0 (N2, q, ^3J = 1.5 Hz), −129.8 (N4), −184.0 (N1, q, ^2J = 1.9 Hz), −331.4 (N5); m/z (FAB^+, xenon, 6 keV, m-NBA matrix), 100 $[MAT + H]^+$; $C_2H_6N_6O_3$ (162.11) calcd: C 14.9, H 3.7, N 51.8%; found: C 14.7, H 3.6, N 51.6%.

Synthesis of 1-Methyl-5-aminotetrazolium Perchlorate (4b). A 0.142 g (1.4 mmol) amount of **4** was dissolved in minimal concentrated (72%) perchloric acid The mixture was layered with ether and cooled in the refrigerator overnight to yield colorless plates, which were filtered off and washed with ether. No further purification was necessary. Alternatively, ether can be diffused into the mixture over 2 days, yielding colorless crystals suitable for X-ray analysis (0.204 g, 1.0 mmol, 70%): mp 125−128 °C; IR (KBr, cm^{-1}) ν 3411(s), 3300(s), 3269(s), 3187(s), 3043(w), 1702-(s), 1684(s), 1603(w), 1325(m), 1280(w), 1072(s), 1033(s), 935-(w), 724(w), 697(m); Raman (200 mW, 25 °C, cm^{-1}) ν 3265(7), 3044(9), 2965(22), 1706(16), 1605(11), 1518(14), 1455(12), 1430-(27), 1331(12), 1282(27), 1230(9), 1149(12), 1088(16), 1052(19), 1022(9), 974(11), 938(100), 782(88), 671(17), 632(25), 468(27), 457(33), 298(24), 226(18); ^{1}H NMR (DMSO-d_6, 25 °C) δ 8.4 (N-H, NH_2) 3.7(−CH_3); ^{13}C NMR (DMSO-d_6, 25 °C) δ 155.2 (C_{arom}), 31.6 (CH_3); ^{15}N NMR (DMSO-d_6, 25 °C) δ −17.3 (N3), −24.2 (N2, q, ^3J = 1.9 Hz), −138.4(N4), −183.8 (N1, q, ^2J = 1.9 Hz), −329.4(N5); ^{35}Cl NMR (DMSO-d_6, 25 °C) δ 1.0 (Cl); m/z (FAB^+, xenon, 6 keV, m-NBA matrix) 100 $[MAT + H]^+$; $C_2H_6N_5O_4Cl$ (199.56) calcd: C 12.0, H 3.0, N 35.1%; found: C 12.0, H 3.0, N 35.1%.

Synthesis of 1,4-Dimethyl-5-aminotetrazolium Iodide (5a). Compound **5a** was synthesized according to a literature procedure with an improved yield of 91%.[5c]

Synthesis of 1,4-Dimethyl-5-aminotetrazolium Nitrate (5b). To a solution of 2.41 g of **5a** (10 mmol) in 10 mL methanol were added 1−2 drops of concentrated nitric acid and 1.70 g (10.0 mmol) of solid silver nitrate. The resulting methanolic suspension was stirred for 3 h under exclusion of light and then filtered through a ~2 cm plug of wet (methanol) packed celite to remove the precipitated silver iodide. The remaining solid was washed twice with methanol. The solution was then transferred to a pear-shaped flask and evaporated nearly to dryness. The resulting solids were recrystallized from 3 mL of boiling methanol (1.2 g, 6.8 mmol, 68%): mp 181−183 °C; IR (KBr, cm^{-1}) ν 3276(s), 3223(s), 3166-(s), 3040(s), 2824(w), 2753(w), 2690(w), 2340(w), 1685(s), 1543-(m), 1424(m), 1396(m), 1307(s), 1196(m), 1058(w), 1038(m), 781(m), 709(w); Raman (200 mW, 25 °C, cm^{-1}) ν 3041(17), 3013-(16), 2959(52), 1699(9), 1544(12), 1457(18), 1428(20), 1400(19), 1359(26), 1259(9), 1041(96), 1011(9), 947(5), 853(7), 792(100), 716(11), 681(7), 631(11), 598(32), 429(11), 325(28), 270(16), 128-(17); ^{1}H NMR (DMSO-d_6, 25 °C) δ 9.2 (s, NH_2) 3.8 (s, CH_3); ^{13}C NMR (DMSO-d_6, 25 °C) δ 148.9 (C_{arom}), 34.2 (CH_3); ^{15}N NMR (DMSO-d_6, 25 °C) δ 4.3 (N6), −29.6 (N2, N3, q, ^3J = 1.9 Hz), −182.8 (N1, N4, q, ^2J = 2.0 Hz), −320.3 (N5); m/z (FAB^+, xenon, 6 keV, m-NBA matrix) $[DMAT]^+$ 114; $C_3H_8N_6O_3$ (176.13) calcd: C 20.5, H 4.6, N 47.7%; found: C 20.5, H 4.3, N 48.0%.

Synthesis of 1,4-Dimethyl-5-aminotetrazolium Perchlorate (5c). To 20 mL methanol was added 4.820 g (20.0 mmol) **5a**. The solution was stirred until all solid had dissolved. A second solution containing 4.140 g of anhydrous silver perchlorate (weighed out in a drybox) dissolved in 5 mL of methanol was added to the solution of **5a** in methanol. Yellow silver iodide precipitated immediately, and the temperature of the reaction mixture rose to the boiling point of methanol. After stirring for 30 min under exclusion of light, the solution was filtered, divided into 12 equal portions, and recrystallized by diffusion of ether into the methanol solutions, yielding clear colorless crystals suitable for X-ray structure determination. No further purification was necessary (2.812 g, 18.0 mmol, 90%): mp 218−223 °C; IR (KBr, cm^{-1}) ν 3384(s), 3331(s), 3268(s), 3193(s), 2670(w), 2480(w), 2046(w), 1688(s), 1545(m), 1454(w), 1258(w), 1108(s), 1053(s), 934(w), 778(w), 625-(m); Raman (200 mW, 25 °C, cm^{-1}) ν 3200(6), 3043(9), 3017-(11), 2957(39), 1695(12), 1546(11), 1453(19), 1436(11), 1419(10), 1397(18), 1358(23), 1049(16), 935(100), 790(99), 626(13), 597-(27), 461(23), 307(25), 273(15); ^{1}H NMR (DMSO-d_6, 25 °C) δ 9.1 (s, NH_2) 3.8 (s, CH_3); ^{13}C NMR (DMSO-d_6, 25 °C) δ 148.5 (C_{arom}), 34.0 (CH_3); ^{15}N NMR (DMSO-d_6, 25 °C) δ 29.5 (N2, N3, q, ^{3}J = 1.9 Hz), −182.8 (N1, N4, q, ^2J = 1.9 Hz), −320.0 (N5); ^{35}Cl NMR (DMSO-d_6, 25 °C) δ 1.0(Cl); m/z (FAB^+, xenon, 6 keV, m-NBA matrix) $[DMAT]^+$ 114; $C_3H_8N_5O_4Cl$ (213.58) calcd: C 16.9, H 3.8, N 32.8%; found: C 16.9, H 3.7, N 32.9%.

Synthesis of 1,4-Dimethyl-5-aminotetrazolium Azide (5d). Method 1. To a suspension of 0.200 g (2.5 mmol) of potassium azide in 2 mL of methanol was added 0.430 g (2.0 mmol) of **5c**. The mixture (suspension) was covered and stirred for 3 h. A white solid was then filtered off, and the remaining solution was divided into two equal portions. Diethyl ether was allowed to diffuse into both solutions over 2 days, yielding clear prismic crystals suitable for X-ray structure determination. No further purification was necessary (0.258 g, 1.7 mmol, 68%).

Method 2. Alternatively, to a solution of 0.240 g (1.0 mmol) of **5a** in 3 mL of methanol was added 0.200 g (1.33 mmol) of silver azide. This suspension was stirred under exclusion of light for 1 h and then filtered. The remaining solution was divided into three 1 mL portions into which diethyl ether was allowed to diffuse over several days yielding identical clear, prismic crystals equally suitable

(14) Stadler, C.; Daub, J.; Koehler, J.; Saalfrank, R. W.; Coropceanu, V.; Schuenemann, V.; Ober, C.; Trautwein, A. X.; Parker, S. F.; Poyraz, M.; Inomata, T.; Cannon, R. D. *J. Chem. Soc., Dalton Trans*. **2001**, *22*, 3373−3383.

for X-ray crystal structure determination. No further purification was necessary (0.122 g, 0.78 mmol, 78%): mp 178−180 °C; IR (KBr, cm^{-1}) ν 3397(w), 3336(w), 2874(s,b), 2024(s), 1689(s), 1535(w), 1459(m), 1426(w), 1392(w), 1330(m), 1204(w), 1067(w), 1037(w), 1009(w), 787(m), 677(w), Raman (200 mW, 25 °C, cm^{-1}) ν 3016(38), 2947(63), 2829(12), 2027(4), 1711(7), 1658(6), 1536(10), 1451(21), 1395(13), 1356(32), 1331(77), 1263(6), 1238(7), 1131(4), 1061(9), 1010(6), 942(7), 792(100), 597(19), 522(10), 464(9), 328(50), 311(20), 289(15), 272(15), 165(29); ^{1}H NMR (DMSO-d_6, 25 °C) δ 8.4 (s, NH_2), 3.8 (s, CH_3); ^{13}C NMR (DMSO-d_6, 25 °C) δ 148.8 (C_{arom}), 33.4 (CH_3); ^{15}N NMR (DMSO-d_6, 25 °C) δ −30.7 (N2, N3, q, ^3J = 1.9 Hz), −133.4 (N7), −185.8 (N1, N4, q, ^2J = 1.9 Hz), −277.1 (N6, N8), −307.2 (N5); m/z (FAB^+, xenon, 6 keV, m-NBA matrix) $[DMAT]^+$ 114; $C_3H_8N_8$ (156.15 g/mol) calcd: C 23.1, H 5.2, N 71.8%; found: C 23.1, H 4.8, N 71.8%.

Synthesis of 1,4-Dimethyl-5-aminotetrazolium Dinitramide (5e). Method 1. To a suspension of 0.220 g (1.5 mmol) of potassium dinitramide in 2 mL of methanol was added 0.210 g (1.0 mmol) of **5c**. The suspension was stirred for 3 h and then filtered. The resulting clear yellow solution was divided into two equal portions, and diethyl ether was allowed to diffuse into the methanol solutions overnight, yielding clear colorless crystals suitable for X-ray structure determination (0.220 g, 1.0 mmol, 67%).

Method 2. Alternatively, to a suspension of 0.370 g (1.0 mmol) of silver bis-pyridine dinitramide in 2 mL of methanol was added 0.240 g (1.0 mmol) of **5a**. The mixture was stirred under exclusion of light for 30 min, the silver iodide was then removed by filtration, the remaining clear, yellow solution was divided into two equal fractions, and diethyl ether was allowed to diffuse into the solutions overnight, yielding clear, colorless needles (0.157 g, 0.71 mmol, 71%): mp 120−122 °C; IR (KBr, cm^{-1}) ν 3341(s), 3314(s), 3254(s), 3139(s), 1683(s), 1525(m), 1502(m), 1443(m), 1430(m), 1327(w), 1249(w), 1163(m), 1046(w), 1006(m), 758(w); Raman (200 mW, 25 °C, cm^{-1}) ν 3049(11), 2963(41), 1689(13), 1526(16), 1425(24), 1397(16), 1353(25), 1329(82), 1252(10), 1182(11), 1046(12), 973(16), 955(15), 825(29), 787(100), 739(7), 594(22), 485(23), 396(12), 313(29), 273(21), 183(14); ^{1}H NMR (DMSO-d_6, 25 °C) δ 9.1 (s, NH_2), 3.9 (s, CH_3); ^{13}C NMR (DMSO-d_6, 25 °C) δ 148.5 (C_{arom}), 34.0 (CH_3); ^{15}N NMR (DMSO-d_6, 25 °C) δ −10.1 (N6,-N8), −29.3 (N2, N3, q, ^3J = 1.9 Hz), −153.0 (N7), −182.6 (N1, N4, q, ^2J = 1.9 Hz), −320.1 (N5); m/z (FAB^+, xenon, 6 keV, m-NBA matrix) $[DMAT]^+$ 114; $C_3H_8N_8O_4$ (220.15) calcd: C 16.4, H 3.7, N 50.1%; found: C 16.3, H 3.9, N 49.9%.

X-ray Crystallography. Crystals were obtained as described above. The X-ray crystallographic data for **4a** were collected on an Enraf-Nonius Kappa CCD diffractometer. Data sets for **4b**, **5b**, **5d**, and **5e** were collected on an Oxford Diffraction Xcalibur 3 diffractometer equipped with a CCD detector. Data for **5c** were collected on a STOE IPDS diffractometer. All data were collected using graphite-monochromated Mo Kα radiation (λ = 0.71073 Å). No absorption corrections were applied to data sets collected for **4a**, **4b**, **5c**, **5d**, or **5e**. A multiscan numerical absorption correction was applied to data collected for **5b** using the ABSPACK[15a] software supplied by Oxford Diffraction. All structures were solved by direct methods (SHELXS-97 and SIR97) [15b,c] and refined by means of full-matrix least-squares procedures using SHELXL-97.

(15) (a) Oxford Diffraction. ABSPACK, CrysAlis CCD and CrysAlis RED. Versions 1.171. Oxford Diffraction Ltd, Abingdon, Oxfordshire, England, 2006. (b) Programs for Crystal Structure Analysis (Release 97−2). Sheldrick, G.M., Institüt für Anorganische Chemie der Universität, Tammanstrasse 4, D-3400 Göttingen, Germany, 1998. (c) Altomare, A.; Burla, M. C.; Camalli, M.; Cascarano, G. L.; Giacovazzo, C.; Guagliardi, A.; Moliterni, A. G. G.; Polidori, G.; Spagna, R. *J. Appl. Crystallogr.* **1999**, *32*, 115−119.

Table 1. Crystallographic Data and Structure Determination Details for **4a** and **4b**

	4a	**4b**
formula	$C_2H_6N_5^+NO_3^-$	$C_2H_6N_5^+ClO_4^-$
formula weight (g/mol)	162.13	199.57
crystal system	monoclinic	monoclinic
space group	$P2_1/n$	$P2_1/n$
a (Å)	10.6122(3)	5.2741(8)
b (Å)	5.3606(2)	20.696(3)
c (Å)	11.5508(4)	7.149(2)
α (deg)	90	90
β (deg)	97.663(2)	106.60(2)
γ (deg)	90	90
V (Å^3)	651.23(4)	747.8(2)
Z	4	4
ρ_{calcd} (g/cm^3)	1.653	1.773
μ (mm^{-1})	0.149	0.499
λ (Mo Kα, Å)	0.71073	0.71073
T (K)	200(2)	200(2)
reflections collected	8969	3813
independent reflections	1484	1465
R_{int}	0.0554	0.0372
observed reflections	1150	1333
F(000)	336	408
R_1[a]	0.0355	0.0484
wR_2[b]	0.1017	0.1061
weighting scheme[c]	0.0483, 0.1647	0.0267, 1.2214
GOOF	1.076	1.161
number of parameters	125	133
CCDC number		

[a] $R_1 = \Sigma||F_o| - |F_c||/\Sigma|F_o|$. [b] $R_w = [\Sigma(F_o^2 - F_c^2)/\Sigma w(F_o)^2]^{1/2}$. [c] $w = [\sigma_c^2(F_o^2) + (xP)^2 + yP]^{-1}$, $P = (F_o^2 - 2F_c^2)/3$.

In the cases of **5b** and **5e**, which crystallize in the non-centrosymmetric space group $P2_12_12_1$, the Friedel pairs were averaged since no meaningful information about absolute structure configuration was obtained. Crystallographic data are summarized in Tables 1 and 2. Selected bond lengths and angles are reported in Table 4 and hydrogen-bonding geometries in Table 5. All non-hydrogen atoms were refined anisotropically. For **4a**, **4b**, **5b**, **5c**, and **5d**, all hydrogen atoms were located from difference Fourier electron-density maps and refined isotropically. In the case of **5e**, the hydrogen atoms of the methyl groups were inserted at idealized positions and were subsequently refined riding on the atom to which they were bonded (fixed isotropic temperature factors with the value of 1.5 *B*eq). Crystallographic data in CIF format are available as Supporting Information.

Results and Discussion

Synthesis. 4 was prepared by methylation of the sodium salt of 5-aminotetrazole with methyl iodide or dimethyl sulfate as described in literature.[14] **4a** and **4b** were prepared by protonation of 4 with the corresponding acid. Several attempts were made to prepare $[HMAT]^+[N_3]^-$ none of which were successful. The failure to form an azide salt is in keeping with N4 acid−base trends in nitrogen-rich heterocycles as discussed in ref 5a. As a consequence, **5a** was prepared by regioselective methylation of **4** at N4 in acetonitrile with excess methyl iodide by a method analogous to that used for the preparation of the iodide salt of **3**.[5a] The salts of **5** were generally prepared by exchange of iodide for nitrate, perchlorate, azide, or dinitramide using the respective silver salt of the desired anion. In the cases of **5d** and **5e**, alternate synthetic routes were also explored because of the sensitivity of the silver salts of azide and dinitramide. In these cases, **5c** was treated with the potassium salt of the

Table 2. Crystallographic Data and Structure Determination Details for **5a**−**e**

	5a[d]	**5b**	**5c**	**5d**	**5e**
formula	$C_3H_8N_5^+I^-$	$C_3H_8N_5^+NO_3^-$	$C_3H_8N_5^+ClO_4^-$	$C_3H_8N_5^+N_3^-$	$C_3H_8N_5^+N_3O_4^-$
mass (g/mol)	241.03	176.15	213.59	156.17	220.17
crystal system	orthorhombic	orthorhombic	monoclinic	orthorhombic	orthorhombic
space group	*Fddd*	$P2_12_12_1$	$P2_1/n$	*Fddd*	$P2_12_12_1$
a (Å)	13.718(2)	5.3855(2)	5.7280(7)	12.351(2)	5.3985(6)
b (Å)	14.486(2)	10.8511(5)	10.9681(8)	13.952(2)	12.926(2)
c (Å)	16.281(2)	12.9152(6)	13.499(2)	17.180(2)	13.336(2)
α (deg)	90	90	90	90	90
β (deg)	90	90	92.24(2)	90	90
γ (deg)	90	90	90	90	90
V (Å^3)	3235.4(5)	754.75(6)	847.4(2)	2960.5(4)	930.6(2)
Z	16	4	4	16	4
ρ_{calcd} (g/cm^3)	1.979	1.550	1.674	1.403	1.572
μ (mm^{-1})	3.891	0.135	0.446	0.106	0.14
λ (Mo Kα, Å)	0.71073	0.71073	0.71073	0.71073	0.71073
T (K)	200(2)	100(2)	200(2)	200(2)	200(2)
reflns collected	6527	4277	7096	6973	4786
indep reflns	964	1290	2001	730	1087
R_{int}	0.036	0.0432	0.0438	0.062	0.062
obsd reflns	786	886	1391	725	973
F(000)	1824	368	440	1312	456
R_1[a]	0.0169	0.0367	0.0333	0.0409	0.0488
wR_2[b]	0.0352	0.0903	0.0801	0.1069	0.1257
weighting scheme[c]	0.0137, 3.5456	0.0503, 0.0000	0.0469, 0.0000	0.0579, 2.4663	0.0762, 0.0516
GOOF	1.128	0.969	0.897	1.165	1.087
no. of parameters	59	141	150	69	146

[a] $R_1 = \Sigma||F_o| - |F_c||/\Sigma|F_o|$. [b] $R_w = [\Sigma(F_o^2 - F_c^2)/\Sigma w(F_o)^2]^{1/2}$. [c] $w = [\sigma_c^2(F_o^2) + (xP)^2 + yP]^{-1}$, $P = (F_o^2 - 2F_c^2)/3$. [d] From ref 5c.

Table 3. ^{15}N and ^{13}C Chemical Shifts (ppm) and Protonation (PIS)/Methylation (MIS) Induced Shifts[a]

	N1	**N2**	**N3**	**N4**	**N5**	C5[j]	C1/C4[j]
1[b,h]	−137.1	−13.1	−13.1	−137.1	−338.9	157.2	
1a[c,h]	−165.2 (−28.1)	−24.5 (−11.4)	−24.5 (−11.4)	−165.2 (−28.1)	−329.1 (9.8)	152.4	
2[d,h]	−167	−5.5	−20.8	−97.5	−338.3	155	
2a[e,i,h]	−164.9 (2.1)	−21.9 (−16.4)	−33.1 (−12.3)	−170.4 (−72.9)	−333.3 (5.0)	152.8	
3a[f,h]	−167.9 (−0.9)	−24.0 (−18.5)	−35.3 (−14.5)	−186.0 (−88.5)	−319.0 (19.3)	148.1	33.6
4[h]	−185	−23.2	2.2	−92.7	−338.2	156.4	32.0
4a[h]	−184 (1.0)	−24 (−0.8)	−13.5 (−15.7)	−129.7 (−37.0)	−331.4 (6.8)	153.6	32.9
4b[h]	−183.8 (1.2)	−24.3 (−1.1)	−17.4 (−19.6)	−139.1 (−46.4)	−329.5 (8.7)	155.2	31.6
5a[g,i]	−182.9 (2.1)	−29.9 (−6.7)	−29.9 (−32.1)	−182.9 (−90.2)	−318.0 (20.2)	149.1	34.7
5b[h]	−182.8 (2.2)	−29.5 (−6.3)	−29.5 (−31.7)	−182.8 (−90.1)	−320.4 (17.8)	148.9	34.2
5c[h]	−182.9 (2.1)	−29.5 (−6.3)	−29.5 (−31.7)	−182.9 (−90.2)	−320.0 (18.2)	148.5	34.0
5d[h]	−185.8 (−0.8)	−30.7 (−7.5)	−30.7 (−32.9)	−185.8 (−93.1)	−307.2 (31)	148.8	33.4
5e[h]	−182.7 (2.3)	−29.4 (−6.2)	−29.4 (−31.6)	−182.7 (−90)	−320.1 (18.1)	148.5	34.0

[a] PIS and MIS shifts in parentheses. [b] From ref 5a. [c] 5-Amino-1*H*-tetrazolium nitrate from ref 5a. [d] From ref 5a. [e] 1,5-Diamino-1*H*-tetrazolium nitrate from ref 5a. [f] 1,5-Diamino-4-methyl-1*H*-tetrazolium Iodide from ref 5a. [g] 1,4-Dimethyl-5-amimotetrazolium iodide from ref 5c. [h] DMSO-d_6. [i] CD_3OD. [j] ^{13}C NMR shifts.

desired anion, thus precipitating potassium perchlorate and avoiding the need to handle highly sensitive, explosive materials. In all cases (protonation by mineral acid or exchange of iodide) the desired compounds were obtained in good to excellent yields with excellent purity. All compounds can be easily recrystallized by the diffusion of diethyl ether into concentrated methanol solutions overnight.

Vibrational Spectroscopy. All salts of **4** and **5** were qualitatively identified by vibrational spectroscopy (infrared and Raman). The infrared and Raman spectra of **4** are in perfect agreement with those reported in literature.[16] All spectra measured showed the characteristic bands of the respective energetic anions (nitrate, perchlorate, azide, and dinitramide). The nitrate anion, NO_3^-, shows a strong, broad IR absorption centered at ∼1350 cm^{-1} and a sharp band near 1050 cm^{-1} in the Raman.[17] Compounds **4a** and **5b** show a broad IR signal masked by cation absorptions with maxima at 1312 cm^{-1} and 1307 cm^{-1}, respectively. In the Raman sharp, intense NO_3^- bands are observed in **4a** and **5b** at 1049 cm^{-1} and 1041 cm^{-1}, respectively, as expected. Salts of the perchlorate anion, ClO_4^-, show a strong broad stretch with its maximum around 1090 cm^{-1} in the infrared spectra and strong, sharp bands around 940 and 460 cm^{-1} in the Raman spectra.[18] As in the cases of **4a** and **5b**, the perchlorate stretch in the IR spectra of **4b** and **5c** is masked to a certain extent by tetrazolium cation absorptions with two strong absorptions appearing in each spectrum at 1072 and 1033 cm^{-1} and 1108 and 1053 cm^{-1}, respectively. Once again, Raman spectroscopy unambiguously confirms the presence of the perchlorate

(16) (a) Bigotto, A.; Klingendrath, R. *Spectrochim. Acta*. **1990**, *46A*, 1683−1692. (b) Levchik, S. V.; Balabanovich, A. I.; Ivashkevich, O. A.; Lesnikovich, A. I.; Gaponik, P. N.; Costa, L. *Thermochim. Acta* **1993**, *225*, 53−65.

(17) (a) Williamson, K.; Li, P.; Devlin, J. P. *J. Chem. Phys.* **1968**, *48*, 3891−3896. (b) Fernandes, J. R.; Ganguly, S.; Rao, C. N. R. *Spectrochim. Acta* **1979**, *35A*, 1013−1020.

Table 4. Selected Bond Lengths (Å) and Angles (deg) in Compounds **4a,b** and **5a**−**e**

	4a	4b	5a[a]	5b	5c	5d	5e
			Bond Lengths				
N1−C5	1.3386(19)	1.337(3)	1.330(3)	1.338(3)	1.328(2)	1.3373(15)	1.341(4)
N1−N2	1.3652(17)	1.370(3)	1.358(3)	1.362(2)	1.359(2)	1.3640(15)	1.356(4)
N1−C1	1.457(2)	1.463(4)	1.451(4)	1.450(3)	1.452(2)	1.4530(18)	1.466(4)
N2−N3	1.2739(18)	1.274(4)	1.277(5)	1.270(3)	1.274(2)	1.268(2)	1.270(4)
N3−N4	1.3604(18)	1.352(4)	1.358(3)	1.367(2)	1.361(2)	1.3640(15)	1.372(4)
N4−C5	1.3364(19)	1.337(4)	1.330(3)	1.337(3)	1.335(2)	1.3373(15)	1.345(4)
N5−C5	1.3173(19)	1.311(4)	1.311(4)	1.315(3)	1.314(3)	1.311(2)	1.304(4)
N4−R[b]	0.93(2)	0.84(4)	1.451(4)	1.458(3)	1.456(3)	1.4530(18)	1.452(4)
			Bond Angles				
C5−N1−N2	109.54(12)	109.6(2)	109.99(19)	109.32(17)	109.70(15)	109.31(11)	110.0(3)
C5−N1−C1	129.16(14)	129.6(3)	128.79(19)	129.64(19)	128.81(16)	128.80(12)	127.4(3)
N2−N1−C1	121.18(13)	120.7(3)	121.2(2)	121.02(19)	121.45(17)	121.65(11)	122.2(3)
N3−N2−N1	108.00(12)	107.7(2)	107.75(13)	108.52(17)	108.01(16)	108.22(7)	108.6(3)
N2−N3−N4	108.02(12)	108.1(2)	107.75(13)	107.77(17)	107.91(14)	108.22(7)	107.6(3)
C5−N4−N3	109.84(13)	110.3(2)	109.99(19)	109.58(18)	109.43(15)	109.31(11)	109.7(3)
N5−C5−N4	127.89(14)	128.2(3)	127.73(12)	127.7(2)	127.61(18)	127.54(8)	127.7(3)
N5−C5−N1	127.50(14)	127.6(3)	127.73(12)	127.5(2)	127.44(17)	127.54(8)	128.3(3)
N4−C5−N1	104.60(13)	104.3(2)	104.5(2)	104.80(19)	104.95(15)	104.92(15)	104.1(3)
C5−N4−R[b]			128.79(19)	128.13(19)	128.90(17)	128.80(12)	128.9(3)
N3−N4−R[b]			121.2(2)	122.25(18)	121.60(15)	121.65(11)	121.3(3)

[a] From ref 5c. [b] R = H (**4a**,**b**) and R = CH_3 (**5a**−**e**).

Table 5. Hydrogen-Bonding Geometry in **4a**,**b** and **5a**−**e**

D−H···A (deg)[b]	D−H (Å)	H···A (Å)	D···A (Å)	D−H···A (deg)
		4a		
N5−H51···O2	0.88(2)	2.352(19)	3.1215(18)	146.1(15)
N5−H51···O2^{i}	0.88(2)	2.369(19)	3.1106(18)	142.1(15)
N5−H52···O1^{ii}	0.88(3)	2.60(3)	3.3606(18)	145(2)
N5−H52···O3^{i}	0.88(3)	2.63(2)	3.0697(17)	111.7(19)
N5−H52···O3^{ii}	0.88(3)	2.17(3)	3.0176(19)	161(2)
N4−H4···O1	0.93(2)	1.74(2)	2.6598(17)	169.3(18)
N4−H4···O2	0.93(2)	2.41(2)	3.0741(17)	128.5(15)
		4b		
N4−H4···O1^{vi}	0.84(4)	2.28(4)	2.952(4)	137(3)
N4−H4···O2^{vii}	0.84(4)	2.51(4)	3.009(4)	119(3)
N4−H4···O2^{v}	0.84(4)	2.29(4)	2.929(3)	133(3)
N5−H52···O1^{iv}	0.77(4)	2.34(4)	3.020(4)	149(3)
N5−H52···O2^{vii}	0.77(4)	2.71(3)	3.152(4)	118(3)
N5−H52···O2^{v}	0.77(4)	2.65(3)	3.216(4)	132(3)
N5−H51···O4^{iii}	0.84(4)	2.07(4)	2.887(4)	162(4)
		5a[a]		
N5−H51···I^{viii}	0.77(3)	2.87(3)	3.6381(16)	172(3)
		5b		
N5−H51···O2^{ix}	0.84(3)	1.99(3)	2.821(3)	169(2)
N5−H52···O2^{x}	0.86(3)	2.05(3)	2.868(3)	158(3)
N5−H52···O3^{x}	0.86(3)	2.65(3)	3.422(3)	149(3)
		5c		
N5−H51O4^{xi}	0.81(3)	2.13(3)	2.926(2)	171(2)
N5−H52O3^{xii}	0.82(3)	2.12(3)	2.931(2)	171(3)
		5d		
N5−H51···N6^{xiii}	0.909(18)	1.955(19)	2.8429(18)	165.0(18)
		5e		
N5−H51···O4^{xv}	0.86(5)	2.03(4)	2.876(4)	165(4)
N5−H52···N6^{xiv}	0.82(5)	2.21(4)	3.004(4)	161(3)
N5−H51···O4^{xiv}	0.86(5)	2.85(5)	3.034(4)	94(4)

[a] From ref 5c. [b] Symmetry codes for **4a**: (i) $-x, -y+2, -z$; (ii) $x+1/2, -y+3/2, z+1/2$. **4b**: (iii) $x-1, y, z$; (iv) $-x, -y, -z$; (v) $-x+1, -y, -z$; (vi) $x, y, z-1$ (vii) $x-1, y, z-1$. **5a**: (viii) $-x+1, -y, -z+1$. **5b**: (ix) $-x+3/2, -y, z+1/2$; (x) $-x+2, y+1/2, -z+3/2$. **5c**: (xi) $-x, -y+1, -z+2$; (xii) $x+1, y, z$. **5d**: (xiii) $-x+1/2, -y, -z+1/2$. **5e**: (xiv) $x-1/2, -y+3/2, -z$; (xv) $x, y, z-1$.

anion in both **4b** and **5c**, showing strong bands at 938 and 935 cm^{-1} and at 457 and 461 cm^{-1}, respectively. The antisymmetric stretch of ionic azides is observed as a strong absorption at around 2000 cm^{-1} and the symmetric stretch as a weak absorption around 1300 cm^{-1} in the IR. In the Raman only the symmetric stretch is observed for ionic azides as a strong band around 1300 cm^{-1}.[19] Interestingly, in both the IR and Raman spectra of **5d** both azide vibrations are observed (2018 and 1329 cm^{-1} in the IR and 2027 and 1331 cm^{-1} in the Raman). The presence of both bands in both IR and Raman spectra seems to indicate strong cation−anion interactions. The dinitramide anion $N(NO_2)_2^-$ has strong absorptions at around 1530, 1445, 1345, 1183, and 1025 cm^{-1} in the infrared and strong bands in the Raman spectrum at 1335 and 830 cm^{-1}.[20] The IR and Raman spectra of **5e** confirm the presence of the dinitramide anion as indicated by bands at 1529, 1446, 1183, and 1011 cm^{-1} in the IR and bands at 1329 and 825 cm^{-1} in the Raman. The IR and Raman spectra of compounds **4a**,**b** and **5a**−**e** also contain a set of bands that can be assigned to the cations: 3400−3100 cm^{-1} [ν(N−H)], 3000−2850 cm^{-1} [ν(C−H)], ∼1680 cm^{-1} [ν(C1=N5) + δ(N5H_2)], 1550−1350 cm^{-1} [ν-(tetrazole ring), $\delta_{as}(CH_3)$, δ(N4-H)], ∼1380 cm^{-1} [$\delta(CH_3)$], 1350−700 cm^{-1} [ν(N1−C1-N4), ν(N−N), γ(CN), δ(tetrazole ring)], <700 cm^{-1} [δ out-of-plane bend (N−H), ω(N5H_2)].[21]

IR spectroscopy also provides detailed insight into cation structure and interionic interactions including hydrogen bonding, which in turn reflect the properties of the counteranions.[22] A comparison of the IR spectrum of **4** to those of **4a** and **4b** shows substantial changes, shifts, and broadening of the bands observed in **4** when it is protonated at N4. The bands at 3328 and 3151 cm^{-1} in **4** are split and shifted

(18) (a) Cohn, H. *J. Chem. Soc.* **1952**, 4282−4284. (b) Redlich, O.; Holt, E. K.; Biegeleisen, J. *J. Am. Chem. Soc.* **1944**, *55*, 13−16.
(19) Haiges, R.; Schroer, T.; Yousuffudin, M.; Christe, K. O. *Z. Anorg. Allg. Chem.* **2005**, *631*, 2691−2695.
(20) Christe, K. O.; Wilson, W. W.; Petrie, M. A.; Michels, H. H.; Bottaro, J. C.; Gilardi, R. *Inorg. Chem.* **1996**, *35*, 5068−5071.
(21) Colthup, N.B.; Daly, L.H.; Wiberley, S.E. *Introduction to Infrared and Raman Spectroscopy*; Academic Press: Boston, 1990.

to slightly higher wavenumbers in both **4a** (bands at 3357, 3306, 3236, and 3159 cm^{-1}) and **4b** (bands at 3411, 3330, 3269, and 3188 cm^{-1}), indicating a strengthening (shortening) of the N−H bonds in the exocyclic amino group. In the case of **4a**, two broad signals appear at 2620 and 2360 cm^{-1}, indicating the presence of strong hydrogen bonding involving the proton at the N4 position on the tetrazole ring. No such broad, lower energy N−H absorptions are observed for **4b**, indicating that only weaker hydrogen bonding should be observed. Differences in N−H stretching band shifts observed in the IR spectra of **4a** and **4b** also seem to indicate the well-known difference in basicity between nitrate and perchlorate. In **4a** a smaller increase in amino N−H stretching frequencies is observed than in **4b** because the ring proton is more weakly bound in **4a** and therefore places less electronic demand on the amino group. In addition to this effect, stronger hydrogen bonding between the amino group protons and the nitrate anion seem to result in weaker amino N−H bonds in **4a** and thus lower energy amino N−H stretching vibrations than observed in **4b**.

In addition to providing information about hydrogen bonding and N−H bond strengths, IR spectra also indicate other structural differences between neutral **4** and the $HMAT^+$ cation. The IR spectrum of **4** shows a strong band at 1667 cm^{-1} (with a shoulder at 1677 cm^{-1}) and another at 1596 cm^{-1} corresponding to amino group deformation and C═N ring stretch, respectively.[16] In spectra of salts **4a** and **4b** a single, higher energy band corresponding to the coupled amino group deformation and exocyclic C═N stretch is observed at 1687 and 1684 cm^{-1} with a shoulder at 1702 cm^{-1}, respectively, and the C═N ring stretch band is no longer observed. These observations are explained perfectly by the structural changes expected on protonation of the tetrazole ring. The exocyclic C−NH_2 bond length should decrease (increase in stretching energy) and the endocyclic C−N bond length should increase (shift to lower wavenumbers). The observations of hydrogen bond strength and structural changes within the cation are verified by the crystal structures of these two materials (see X-ray discussion).

IR spectra of the salts of **5** also provide insight into the cation structure, hydrogen bonding, and nature of the anions. Quaternization of **4** with methyl iodide yields **5a**. IR spectra show a splitting of the asymmetric amino group stretching absorption observed at 3329 cm^{-1} for **4** into two bands (3249 and 3216 cm^{-1}) for **5a**. The symmetric NH_2 stretch remains a single discrete band shifted to slightly lower energy (3082 cm^{-1}, from 3155 cm^{-1} for **4)** for **5a**. One might expect quaternization of **4** to lead to higher energy NH_2 stretching vibrations in **5a**. However, this is not observed in the case of **5a**. Cation−anion hydrogen-bonding would seem to explain the lower than expected NH_2 stretching energies. Strong cation−anion hydrogen-bonding is observed in the X-ray structure of **5a**.[5c] An overview of the IR spectra of salts of **5** in this study shows that the energies of amino group stretching vibrations are almost entirely dependent on the counteranion. The highest energy NH_2 stretching bands (3378, 3328, 3265, and 3191 cm^{-1}) and thus weakest interionic interactions are observed, as expected, in the perchlorate salt, **5c**. The dinitramide salt, **5e**, exhibits the next highest energy set of NH_2 stretching bands (3341, 3314, 3254, and 3139 cm^{-1}) and thus the next weakest interionic interactions. **5b** exhibits slightly stronger interionic interactions than those observed for **5a** with broader, more intense amino group stretching vibrations appearing at 3276, 3223, 3166, and 3040 cm^{-1}. Last, the NH_2 stretching band in the IR spectrum of **5d** is a broad, intense signal with a maximum at 2874 cm^{-1}, indicating the strongest cation−anion interactions found in for a salt of **5**. The significant strength of the interactions observed in **5d** is also indicated by the above-mentioned observation of the azide group antisymmetric stretch in the Raman spectrum, which, in purely ionic compounds, should not be observed. All of the observations of interionic hydrogen bond stregnth are confirmed by X-ray crystallography.

Further structural comparison of the $HMAT^+$ and $DMAT^+$ cations can be made by IR spectroscopy. The spectra of salts **4a** and **4b** show the above-mentioned coupled amino group deformation exocyclic C═N stretching vibration at 1687 and 1684 cm^{-1}, respectively. The IR spectra of **5a**, **5b**, **5c**, **5d**, and **5e** all show the amino group deformation exocyclic C═N stretching vibration as a single band at 1677, 1685, 1686, 1685, and 1683 cm^{-1}, respectively, indicating that the ring and exocyclic amino group geometries in $HMAT^+$ and $DMAT^+$ should be very similar. Once again, X-ray crystallography confirms this suggestion.

NMR Spectroscopy. All salts and their precursor **4** were fully characterized by multinuclear (^1H, ^{13}C, ^{15}N, and when possible ^{35}Cl) NMR spectroscopy. The chemical shifts recorded for all nuclei as well as ^1J, ^2J, and ^3J ($^1H-^{15}N$) coupling constants are reported in the experimental section. In the case of **4** all recorded signals and $^1J(^1H-^{15}N)$ couplings are in excellent agreement with previously published results[23] and the ^1H and ^{13}C resonances are observed as expected.[14] The $^1J(^1H-^{15}N)$, ^2J, and ^3J coupling constants for **4** (see Experimental Section), reported here for the first time, and those for compounds **4a**, **4b**, and **5a**−**e** are in good agreement with typical values for ^2J and $^3J(^1H-^{15}N)$ coupling constants.[24]

In addition to providing a quick method to uniquely identify the compounds synthesized, protonation (**4a** and **4b**, PIS)- and methylation (**5a**−**e**, MIS)-induced shifts (calculated as a difference in ^{15}N shift between analogous nitrogen signals in neutral **4** and salts of **4** and **5**) can be used to derive information about the structure in solution and hydrogen bonding (interionic interactions). In the literature, PIS and MIS values have shown to be useful in determining unequivocally the site of protonation or methylation for a variety of heterocyclic compounds.[5a,25] So, for salts **4a** and **4b** as well as **5a**−**e**, the substantial protonation- and methylation-induced shifts observed are tabulated in Table

(22) Jeffrey, G. A. *An Introduction to Hydrogen Bonding*; Oxford Univ. Press: New York, 1997.

(23) Bocian, W.; Jazwinski, J.; Kozminski, W.; Stefaniak, L.; Webb, G. A. *J. Chem. Soc., Perkin Trans. 2* **1994**, *6*, 1327−1332.

(24) Martin, G. J.; Martin, M. L.; Gouesnard, J-P. *^{15}N-NMR Spectroscopy*; Springer: Berlin, Germany, 1981.

3 (similar measurements of salts of **2** are shown for comparison).

The PIS data for **4a** and **4b** show, as expected from the literature, the most significantly negative (−37.0 and −46.4 ppm, respectively) shifts at N4, indicating that protonation in solution occurs exclusively at N4. Additionally, slight positive PIS shifts for N5 (6.8 ppm for **4a** and 8.7 ppm for **4b**) show a decrease in electron density at N5 as compared to neutral **4** and thus indicate a strengthening of the C−NH_2 and N−H bonds. Such an observation is in excellent agreement with the solid-state IR and Raman data as discussed above. The differences in cation structure due to differences in counteranion basicity observed in the vibrational spectra are also corroborated by the differences in PIS shifts for **4a** and **4b** at N4 and N5. **4a** shows less dramatic PIS shifts (greater structural similarity to **4**) and thus stronger interactions between $HMAT^+$ (especially the acidic proton at N4) and nitrate than **4b** for which more dramatic PIS shifts (lesser structural similarity to **4**) are observed, indicating weaker cation−anion interactions (hydrogen bonding) in **4b**.

The ^{15}N NMR spectrum of the reaction mixture of **4** with methyl iodide shows only three resonances, thus indicating selective methylation at N4 forming **5a**. In addition, the N1 (the N1 and N4 resonances are the same because of molecular symmetry) resonance observed is identical to that of N1 in **4b** and shows an MIS of −90.2 relative to N4 of **4**. The observed resonances and MIS values observed and calculated for all salts of **5** except for **5d** are all very nearly equal within the tolerances of the measurement. The largest differences in resonances and MIS values are observed for N5, a fact which is explained by the NH_2^+ protons that interact to varying degrees with the counteranions. **5d** shows the strongest cation−anion interactions and thus the largest positive MIS at N5 and slight but significant shifts throughout the entire spectrum. Such shifts for **5d** fit nicely with vibrational data showing strong azide−NH_2^+ interactions in the solid state. For the remaining salts of **5**, the MIS data are less conclusive than vibrational methods, showing only similar amounts of interaction between the cations and anions.

X-ray Structures. All salts of **4** and **5** have been characterized by X-ray structure determination. Crystallographic data and structure determination details are presented in Tables 1 and 2. Selected interatomic distances and angles are shown in Table 4. Additionally, hydrogen bond parameters are tabulated in Table 5. **4a** and **4b** crystallized in the same monoclinic space group $P2_1/n$ but differences in the lengths of the crystallographic axes and monoclinic angles indicate that the packing in the two structures is certainly different. Although both structures are composed of three-dimensional hydrogen-bonded networks consisting of seven crystallographically independent hydrogen bonds each, the packing around the planar nitrate anion in **4a** is, for geometric reasons, different than the packing around the tetrahedral perchlorate anion in **4b**. **5a** and **5d** both crystallize in the orthorhombic space group *Fddd* and are closely related structurally. Both structures crystallize in planar layers within which cations and anions hydrogen bond to one another forming dimeric pairs (two cations and two anions), which interact with one another through nonpolar interaction of the methyl groups (see Figures 1 and 2). Not surprisingly, the *a*-axes in these two structures differ the least (∼0.07 Å) since this is the direction normal to the planar cation−anion layers in both structures, and the only interaction between the layers in both cases are weak van der Waals forces. The *b*- and *c*-axes are slightly more dissimilar (∼0.9 Å and ∼0.5 Å, respectively). However, these differences are easily rationalized, by the different sizes and geometries of the iodide and azide anions. In the case of the monatomic iodide anion in **5a**, the *b*-axis is slightly longer than that of the azide anion in **5d** since iodine has a larger van der Waals radius (2.15 Å) than nitrogen (1.5 Å).[26] For the *c*-axis, the situation is reversed with **5d** having a longer axis than **5a** since the linear azide anions in **5d** are arranged parallel to the *c*-axis. Compound **5c** (Figure 3) also forms dimeric pairs similar to those observed in **5a** and **5d**; however, because of the

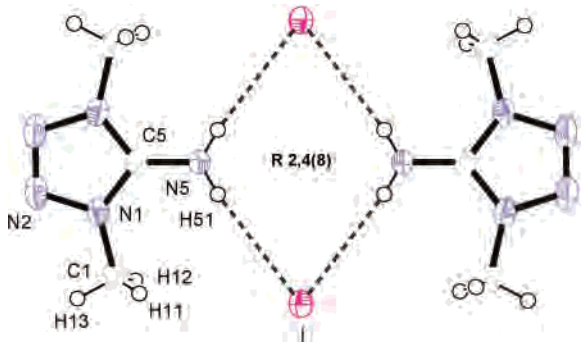

Figure 1. View of a hydrogen-bonded dimer of 1,4-dimethyl-5-aminotetrazolium iodide (**5a**) with atom labels for one asymmetric unit and thermal ellipsoids shown for 50% probability along the crystallographic *a*-axis.

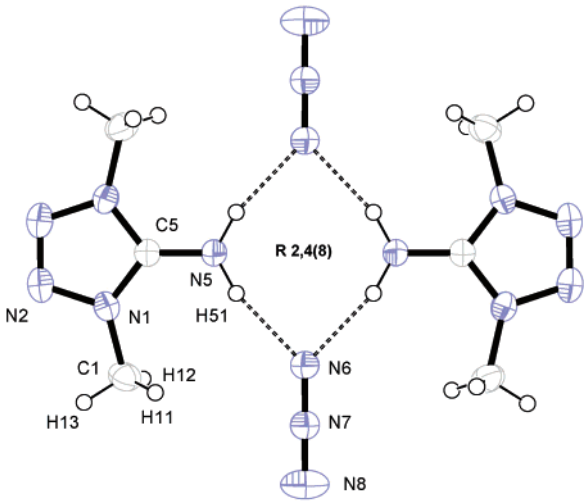

Figure 2. View of a hydrogen-bonded dimer of 1,4-dimethyl-5-aminotetrazolium azide (**5d**) with atom labels for one asymmetric unit and thermal ellipsoids shown for 50% probability along the crystallographic *a*-axis.

(25) (a) Darwich, C.; Karaghiosoff, K.; Klapötke, T. M.; Miró, Sabaté, C. *Z. Anorg. Allg. Chem.* **2007**, in press. (b) Garrone, A.; Fruttero, R.; Tironi, C.; Gasco, A. *J. Chem. Soc., Perkin Trans. 2* **1989**, *12*, 1941−1945.

(26) Wiberg, N. *Holleman-Wiberg, Lehrbuch der Anorganischen Chemie*; Walther de Gruyter: Berlin, 2006.

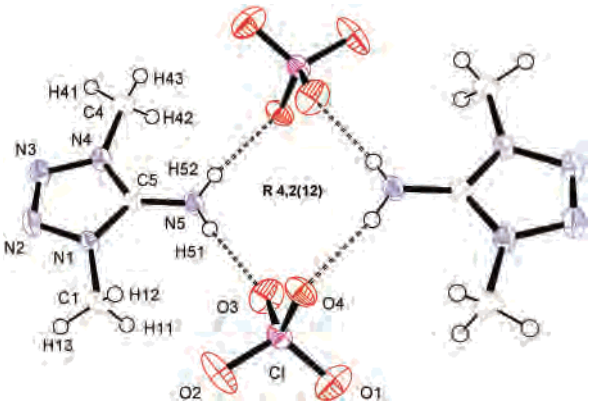

Figure 3. Hydrogen-bonded dimer of 1,4-dimethyl-5-aminotetrazolium perchlorate (**5c**) with atom labels for one formula unit and thermal ellipsoids shown for 50% probability.

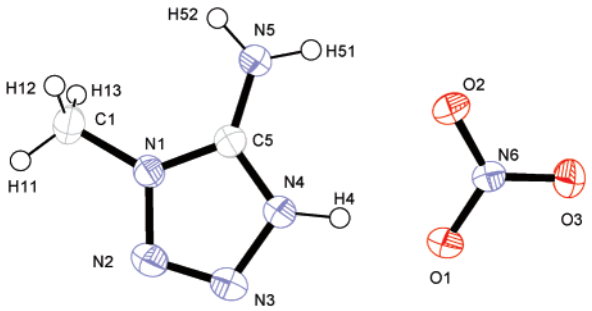

Figure 4. Formula unit of 1-methyl-5-aminotetrazolium nitrate (**4a**) with atom labels and thermal ellipsoids shown for 50% probability.

tetrahedral shape of the perchlorate anion the compound crystallizes in the monoclinic space group $P2_1/n$ rather than the orthorhombic *Fddd*, with substantially different lattice parameters (Table 1). Last, structures **5b** and **5e** both crystallize in the non-centrosymmetric (chiral) monoclinic space group $P2_12_12_1$ with similar lattice parameters. As in the case of **5a** and **5d**, the packing patterns of these two compounds are also related. Both form infinite hydrogen bonded (three H-bonds each, see Table 5), helical (source of chirality) chains of cations and anions. Interactions between the chains are once again limited weak van der Waals interactions. Although the axes are similar, the axis of the helix is parallel to the *a*-axis in **5b** and parallel to the *b*-axis in **5e**.

In the structures of **4a** and **4b** the $HMAT^+$ cations are nearly identical within the limits of structure determination accuracy as suggested by IR and Raman observations. The $HMAT^+$ cation is planar with exception of the methyl group protons which are staggered with respect to the ring in both **4a** and **4b** (Figures 4 and 5). Unfortunately, we were unable to determine the structure of **4** for comparison; however, all bond lengths and angles in **4a** and **4b** are quite similar to those found in analogous salts of **1** and **2**. The differences observed are no greater than 0.01 Å for analogous interatomic distances and no greater than 5° for analogous angles.[5a,b] As in salts of **1** and **2**, protonation is observed exclusively at the N4 position, which is in excellent agreement with NMR observations, and as mentioned above, the only slight variation in the $HMAT^+$ cations observed is in the location of H4. Although the determination of absolute hydrogen atom

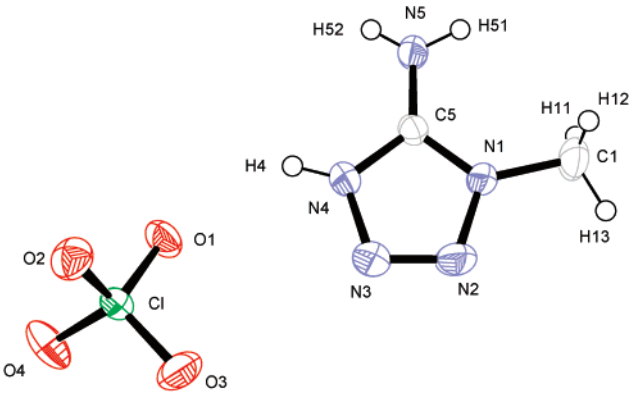

Figure 5. Formula unit of 1-methyl-5-aminotetrazolium perchlorate (**4b**) with atom labels and thermal ellipsoids shown for 50% probability.

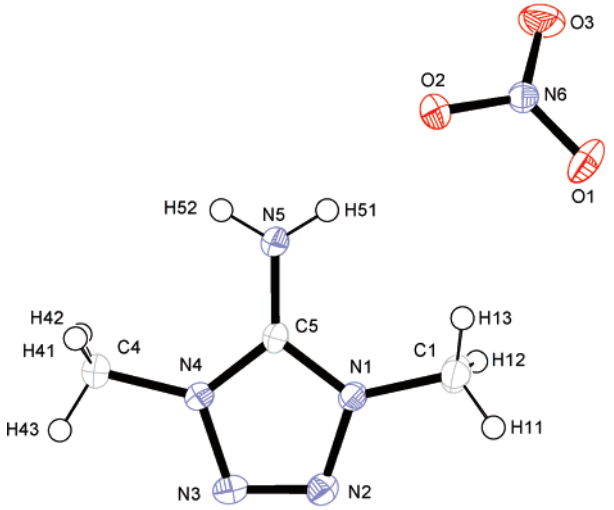

Figure 6. Formula unit of 1,4-dimethyl-5-aminotetrazolium nitrate (**5b**) with atom labels and thermal ellipsoids shown for 50% probability.

position by X-ray methods is prone to large systematic errors stemming from the electronegativity of the atom to which the H atom is bonded,[27] the $HMAT^+$ cations in **4a** and **4b** are very nearly equal, so a comparison of the relative lengths of the N4−H4 bond should provide pertinent information about hydrogen bonding in these structures. Stronger hydrogen bonding is observed in **4a** because the calculated length of the N4−H4 bond (0.93(2) Å) is greater than that of the same bond (0.84(4) Å) in **4b**. As stated above, vibrational spectroscopy, as well as the acid−base properties of nitrate and perchlorate, suggest that exactly such a trend in hydrogen bond strength should be present (a more in depth discussion of hydrogen bonding in all salts of **4** and **5** follows below).

The structures of **5a**−**e** also show nearly identical $DMAT^+$ cations within the structure determination tolerances, and only slight differences in the rotational configuration of the methyl groups are also observed (Figures 1−3, 6, and 7). The geometry of the $DMAT^+$ cations, aside from their higher symmetry, is also very nearly identical to that observed for $HMAT^+$ cations, and they are therefore planar with the exception of the methyl group protons. Only the N5-H calculated distance in the $DMAT^+$ cation of **5d** varies

(27) Jeffrey, G. A.; Lewis, L. *Carbohyd. Res.* **1978**, *60*, 179−182.

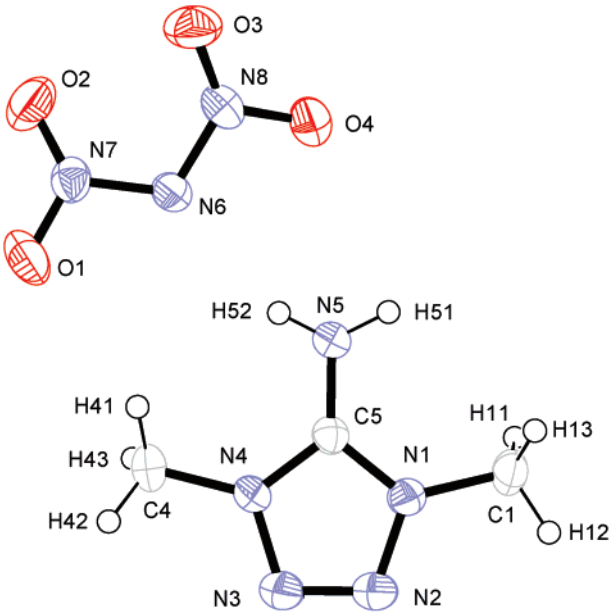

Figure 7. Formula unit of 1,4-dimethyl-5-aminotetrazolium dinitramide (**5e**) with atom labels and thermal ellipsoids shown for 50% probability.

significantly (~0.1 Å) from those found for the other salts of **5**. The formation of strong interionic hydrogen bonds, as observed by both vibrational and NMR spectroscopy, explains this deviation nicely. Last, all of the anions employed in this study are crystallographically identical to those observed in numerous other studies and discussion thereof is thus omitted.

As suggested above, intermolecular (or interionic) hydrogen bonding plays a pivotal role in determining the properties of energetic materials and is also a defining element in the structures of salts of **4** and **5**. As might be expected, salts of **4** show more extensive hydrogen bonding than salts of **5** for the simple reason that more and better proton donors are available in salts of **4**. **4a** and **4b** form seven hydrogen bonds each ranging in strength from strong (D−H···A, 2.660(2) Å) to weak (D−H···A 3.361(2) Å) which, in both cases, form extensive networks within the lattice. The extensive hydrogen bond network is probably responsible for the low sensitivity of **4a** to friction and impact as well as its reasonably high density. Complete description of the reasonably complex hydrogen-bonding networks in **4a** and **4b** is facilitated by the use of graph-set analysis as described by Berstein et al.[28] For **4a**, the computer program *RPLUTO*[29] identifies several characteristic two-bond (binary) ring graph-set patterns including R 2,2(4), R 1,2(6), R 2,2(6), R 2,1(4) as shown in Figure 8. Similarly, the structure of **4b** is characterized by a hydrogen bond network built principally of two hydrogen bond ring R 2,2(4), R 1,2(6), and R 4,4-(12) graph-sets (Figure 9).

As mentioned above, salts of **5** build fewer hydrogen bonds than those of **4**. The most extreme case is that found in **5a**

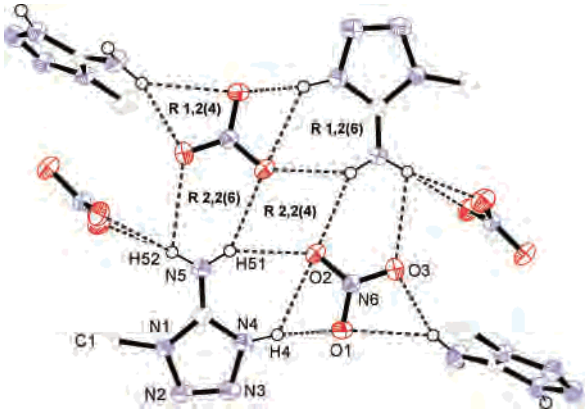

Figure 8. Ring hydrogen-bonding graph sets in 1-methyl-5-aminotetrazolium nitrate (**4a**). Methyl group protons are omitted for clarity.

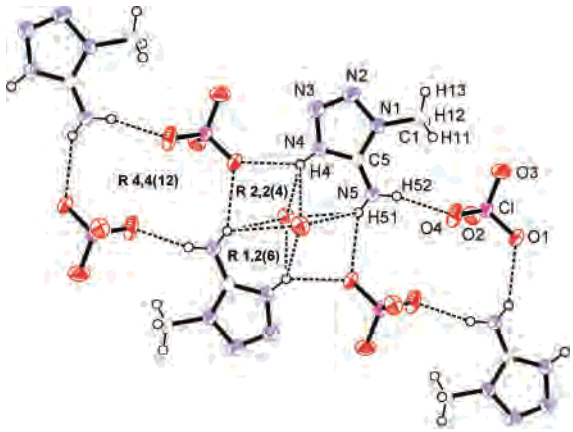

Figure 9. Ring hydrogen-bond graph sets in 1-methyl-5-aminotetrazolium perchlorate (**4b**).

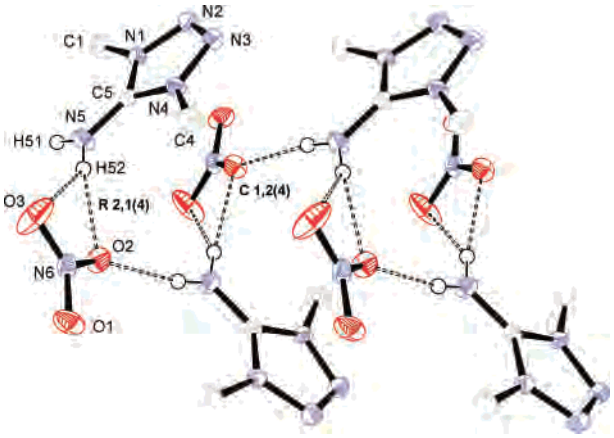

Figure 10. Hydrogen-bonding in 1,4 dimethyl-5-aminotetrazolium nitrate (**5b**) with atom labels and thermal ellipsoids shown for 50% probability. Methyl group protons are omitted for clarity.

and **5d** in which a single, crystallographically independent hydrogen bond, N5−H51···N03, is observed. Because of symmetry, this single hydrogen bond links the planar cation−anion pair dimers forming a common R 2,4(8) motif (Figures 1 and 2). Nonplanar dimeric pairs linked in a ring motif (binary R 4,2(12)) are also observed in the structure of **5c** as seen in Figure 3. In the case of **5b** and **5e**, the infinite helices observed are described as chain graph-sets C 1,2(4) (Figures 10 and 11). The hydrogen bonds composing the helices range in length from short (strong) to medium.

(28) Bernstein, J.; Davis, R. E.; Shimoni, L.; Chang, N-L. *Angew. Chem., Int. Ed. Engl.* **1995**, *34*, 1555−1573.
(29) (a) Motherwell, W. D. S.; Shields, G. P.; Allen, F. H. *Acta. Crystallogr.* **2000**, *B56*, 466−473. (b) Motherwell, W. D. S.; Shields, G. P.; Allen, F. H. *Acta. Crystallogr.* **1999**, *B55*, 1044−1056. (c) http://www.ccdc.cam.ac.uk/support/ documentation/rpluto/TOC.html.

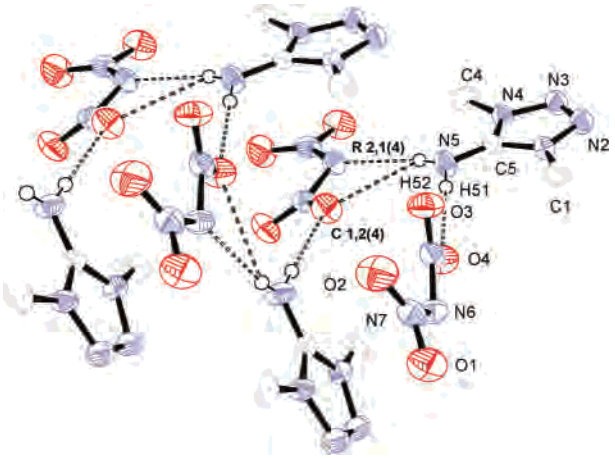

Figure 11. Hydrogen-bonding in 1,4-dimethyl-5-aminotetrazolium dinitramide (**5e**). Methyl group protons are omitted for clarity.

Additionally, in both cases one proton is chelated by the nitrate anion, resulting in an R 2,1(4) ring motif.

Energetic Properties. In order to assess the energetic properties of compounds **4a,b** and **5a**−**e** the thermal stability (melting and decomposition points from DSC measurements), sensitivity to friction, impact, electrostatic discharge, and thermal shock of each salt was experimentally determined (Tables 6 and 7). For each CHNO salt, the heat of combustion was determined experimentally using oxygen bomb calorimetry. The heats and energies of formation were back-calculated from the combustion data and subsequently used in conjunction with the molecular formula and density (from X-ray) to predict the detonation performance parameters (pressure and velocity) for each compound using the EXPLO5 computer code.[30]

DSC measurements were made on samples of ~1 mg of each energetic compound in this study (**4a,b**, **5a**−**e**) and show melting points at or above 120 °C and decomposition points above 170 °C (Table 6). The melting and decomposition points of the salts in this study are generally higher than those for analogous salts of **2** and **3**. In comparison to commonly used explosives like TNT and RDX, the compounds in this study have higher melting points than TNT (81 °C) and lower melting points than RDX (204 °C).[3] Compounds **4a** and **5e** decomposed at a lower temperature than RDX (230 °C), and the remaining energetic compounds decompose at a higher temperature than RDX. Only **5c** exhibits a higher thermal stability than TNT. In addition to DSC analysis, all compounds were tested by placing a small sample (~0.5−1 mg) of compound in the flame. This resulted in an explosion in the case of **4b**, **5c**, and **5e**, and in all other cases, the compound burned or deflagrated without exploding (both TNT and RDX explode under similar conditions). From these "flame test" observations it would seem that the compounds in this study with a less negative oxygen balance were more sensitive to thermal shock as might be expected.

Data collected for friction, impact, and electrostatic discharge sensitivity testing are summarized in Table 7. The compounds in this study are significantly less sensitive to friction and impact than analogous salts of **2** and **3**. Within the series of salts based on **4** and **5**, the trend of increasing sensitivity with decreasingly negative oxygen balance is observed as was the case for the "flame test." Also, each compound was roughly tested for sensitivity to electrostatic discharge by spraying sparks across a small (three to five crystals) sample of material using a tesla coil (ESD testing). All compounds except **4b** failed to explode under these conditions. Once again, a comparison with the properties of TNT and RDX is useful to assess the energetic salts in this study. Compounds **4a**, **5b**, and **5d** are less sensitive to both friction and impact than TNT (15 J) and RDX (7.4 J).[3] All compounds in this study were less sensitive to friction than TNT, and except **4b** all compounds are less sensitive to electrostatic discharge than both TNT and RDX. Last, all of the compounds in this study, except **4b**, are safe for transport under the UN Recommendations on the Transport of Dangerous Goods as described in ref 31.

In addition to safety considerations, performance of new energetic materials is of utmost interest. Using the molecular formula, density (from X-ray) and energy of formation (ΔU_f), the EXPLO5 computer code can be used to calculate the detonation velocity and pressure of CHNO explosives. For several reasons, the performance of the perchlorate-containing salts **4b** and **5c** was not assessed. First, it was not possible to obtain sets of combustion measurements within which reasonable agreement between individual measurements was observed. Second, the methods used in this study for detonation parameter approximation (EXPLO5 and Kamlet and Jacobs equations) are not designed for use with halogen-containing compounds. Last and most significantly, halogen-containing explosives are of little interest because of the toxic nature of these compounds.

The energies of formation of **4a**, **5b**, **5d**, and **5e** were back-calculated from the heat of combustion on the basis of combustion eqs 1−4, Hess's Law, known standard heats formation for water and carbon dioxide,[32] and a correction for change in gas volume during combustion.

$$[C_2H_6N_5]^+[NO_3]^-(s) + 2O_2 \rightarrow 2CO_2(g) + 3H_2O(l) + 3N_2(g) \quad (1)$$

$$[C_3H_8N_5]^+[NO_3]^-(s) + {}^7/_2O_2 \rightarrow 3CO_2(g) + 4H_2O(l) + 3N_2(g) \quad (2)$$

$$[C_3H_8N_5]^+[N_3]^-(s) + 5O_2 \rightarrow 3CO_2(g) + 4H_2O(l) + 4N_2(g) \quad (3)$$

$$[C_3H_8N_5]^+[N(NO_2)_2]^-(s) + 3O_2 \rightarrow 3CO_2(g) + 4H_2O(l) + 4N_2(g) \quad (4)$$

The experimentally determined heats of combustion and back-calculated energies of formation for compounds **4a**, **5b**, **5d**, and **5e** are tabulated in Table 6 with experimental uncertainties (standard deviations for the sets of five individual measurements). As noted above, the standard

(30) Suceska, M. *Propellants, Explos., Pyrotech.* **1991**, *16*, 197−202.

Table 6. Physical Properties of **4a**,**b** and **5b**−**e**

	4a	**4b**	**5b**	**5c**	**5d**	**5e**
formula	$C_2H_6N_6O_3$	$C_2H_6N_5O_4Cl$	$C_3H_8N_6O_3$	$C_3H_8N_5O_4Cl$	$C_3H_8N_8$	$C_3H_8N_8O_4$
T_m (°C)[a]	162	125	181	225	186	120
T_d (°C)[b]	178	245	270	315	>250	174
N (%)[c]	51.8	35.1	47.7	32.8	71.8	50.9
Ω (%)[d]	−39.5	−20.0	−63.6	−41.2	−102.5	−43.6
ρ (g/cm^3)[e]	1.654	1.773	1.523	1.674	1.403	1.572
$\Delta_c U_{exp}$ (cal/g)[f]	−2510(10)		−3190(30)		−4500(100)	−2570(70)
$\Delta_f U_{exp}$ (kJ/ kg)[g]	−350(60)		160(100)		3800(500)	200(300)

[a] Chemical melting point (DSC onset) from measurement with $\beta = 10$ °C/min. [b] Decomposition point (DSC onset) from measurement with $\beta = 10$ °C/min. [c] Percentage nitrogen. [d] Oxygen balance. [e] Density from X−ray measurements. [f] Experimentally determined (oxygen bomb calorimetry) constant volume energy of combustion. [g] Experimentally determined (back-calculated from $\Delta_c U_{exp}$) energy of formation.

Table 7. Initial Safety Testing Results for **4a**,**b** and **5b**−**e** and Predicted Energetic Performance of **4a**, **5b**, **5d**, and **5e**, Using the EXPLO5 Code

	P_{det} (GPa)[a]	D (m/s)[b]	impact (J)[c]	friction (N)[c]	ESD (±)[d]	thermal shock
4a	25.6	8100	>30	>360	−	burns
4b			3	10	+	explodes
5b	20.2	7500	>30	>360	−	burns
5c			5.5	96	−	deflagrates
5d	21.7	8200	>30	>360	−	burns
5e	21.2	7500	5	360	−	deflagrates

[a] Detonation pressure. [b] Detonation velocity. [c] Impact and friction sensitivities determined by standard BAM methods (see ref 34). [d] Rough sensitivity to 20 kV electrostatic discharge (ESD), + sensitive, − insensitive from an HF-Vacuum-Tester type VP 24.

Table 8. EXPLO5 Predicted Performance of TNT, RDX, and CHNO Salts of DAT and MDAT[c]

	P_{det} (GPa)[a]	D (m/s)[b]
TNT	20.5	7100 (6900)
RDX	34.0	8900 (8700)
2a[d]	31.0 [33.3]	8700 [8800]
3b[e]	20.3 [23.4]	7500 [7700]
3d[f]	21.9 [20.8]	8200 [7400]
3e[g]	28.4 [33.6]	8400 [8800]

[a] Detonation pressure. [b] Detonation velocity. [c] Experimental values in curved brackets and Kamlet and Jacobs predictions from ref 5a in square brackets. [d] 1,5-Diamino-1*H*-tetrazolium nitrate. [e] 1,5-Diamino-4-methyl-1*H*-tetrazolium nitrate. [f] 1,5-Diamino-4-methyl-1*H*-tetrazolium azide. [g] 1,5-Diamino-4-methyl-1*H*-tetrazolium dinitramide.

deviations of the sets of five measurements used to experimentally determine the heat of combustion of each compound are generally quite large. The substantial uncertainties stem from several sources. First, and perhaps most significantly, all compounds in this study contain a large percentage of nitrogen and relatively little carbon or hydrogen; therefore, upon combustion, relatively little energy is released and very sensitive equipment would be required to detect such minute energy changes. To compensate for this, larger sample sizes would seem logical, but for safety reasons as well as practical ones, the use of larger samples is not an effective solution. When larger samples or "concentrated" mixtures of compound and diluting agent (benzoic acid) are used for oxygen bomb calorimetric measurements, the samples tend not to combust cleanly but rather to explode. The explosion results in incomplete combustion and thus to less reliable measurements.

However, it is still possible to reasonably estimate explosion parameters for each compound on the basis of experimentally determined energy of formation for each energetic salt. The EXPLO5 code, using the following values for the empirical constants in the Becker−Kistiakowsky−Wilson equation of state (BKWN-EOS): $\alpha = 0.5$, $\beta = 0.176$, $\kappa = 14.71$, and $\theta = 6620$, was used. The results of the calculations are shown in Table 7 for **4a**, **5b**, **5d**, and **5e**. Table 8 shows the results of EXPLO5 calculations for TNT, RDX, and salts of **2** and **3** analogous to **4a**, **5b**, **5d**, and **5e**. From the EXPLO5 predictions made using the BKWN-EOS parameters given above and the known data for TNT and RDX, it would seem that detonation velocity and most likely pressure as well are slightly overestimated. Taking into account this systematic overestimation, the estimated performance of all of the compounds assessed in this study fall between those of TNT (7100 m/s, 20.5 GPa) and RDX (8900 m/s, 34.0 GPa) (see Tables 7 and 8). In addition, the detonation pressure and velocity of the C−H−N−O salts of **2** and **3** presented in ref 5a were also calculated with EXPLO5 using the same parameters and are summarized in Table 8. Previously reported detonation pressure and velocity predictions of salts of **2** and **3** made using the empirical equations of Kamlet and Jacobs[33] are also shown in Table 8 for comparison to the EXPLO5 results. Compounds **5b** and **5d** are predicted to perform as well as the analogous MDAT salts, and compounds **4a** and **5e** should show slightly lower performance than the analogous DAT and MDAT salts but therefore much lower sensitivities. The better performance (and higher sensitivity) of the DAT salts is most likely due in large part to the higher densities of DAT and MDAT salts.

Conclusion

A new series of energetic salts based on **1** has been synthesized simply from readily available materials in moderate to excellent yields. Each salt was characterized fully, including X-ray structure determination. The hydrogen-bonded networks observed were assessed for strength (IR

(31) Test methods according to the *UN Recommendations on the Transport of Dangerous Goods, Manual of Tests and Criteria*, 4th rev. ed.; United Nations Publication: New York, 2003.
(32) NIST Chemistry WebBook, NIST Standard Reference Database Number 69, March 2003 release, www version: http://webbook.nist.gov/ chemistry/.
(33) Kamlet, Mortimer J.; Jacobs, S. J. *J. Chem. Phys*. **1968**, *48*, 23−35.
(34) Test methods according to the *UN Recommendations on the Transport of Dangerous Goods, Manual of Tests and Criteria*, 4th rev. ed.; United Nations Publication: New York, 2003, ISBN 92-1-139087-7, Sales No. E.03.VIII.2. 13.4.2 Test 3(a)(ii) BAM Fallhammer.

and X-ray) and form (X-ray). **4a** and **5d** show the strongest networks and **4a** and **4b** show the most complex. All salts in this study show good thermal stabilities (decomposition above 170 °C) and, except in the case of **4a**, good separation (∼50 °C) of melting and decomposition points. All compounds in this study, aside from **5d**, have slightly negative oxygen balances. The densities of all of the salts are slightly less than the analogous salts of 1,5-diaminotetrazole, resulting in lower sensitivities to impact and friction but similar predicted performance. All of the compounds, except **4b**, are classified as less sensitive, several qualify as insensitive energetic materials, and all compounds are predicted to perform at least as well as TNT and possibly as well as RDX. Several salts of **1** are promising candidates for further investigation, scale-up, and possible application as less sensitive and insensitive explosives.

Acknowledgment. Financial support of this work by the Ludwig-Maximilian University of Munich (LMU), the Fonds der Chemischen Industrie (FCI), the European Research Office (ERO) of the U.S. Army Research Laboratory (ARL) under contract nos. N 62558-05-C-0027 and 9939-AN-01, and the Bundeswehr Research Institute for Materials, Explosives, Fuels and Lubricants (WIWEB) under contract nos. E/E210/ 4D004/X5143 and E/E210/7D002/4F088 is gratefully acknowledged. The authors also thank Dr. Margaret-Jane Crawford for guidance and many insightful discussions.

Supporting Information Available: Crystallographic data in CIF format. This material is available free of charge via the Internet at http://pubs.acs.org.

IC701832Z